Marchantin A Trimethyl Ether: Its Molecular Structure and Tubocurarine-like Skeletal Muscle Relaxation Activity

Zenei TAIRA,* Masao TAKEI, Koiti ENDO, Toshihiro HASHIMOTO, Yoko SAKIYA, and Yoshinori ASAKAWA

Faculty of Pharmaceutical Sciences, Tokushima Bunri University, Yamashiro-cho, Tokushima 770, Japan.
Received January 28, 1993

Marchantin A is a novel macrocyclic bis(bibenzyl)ether isolated from the liverwort *Marchantia* species. An X-ray study of its derivative, marchantin A trimethyl ether, revealed that the molecule possesses convex and concave surfaces, with a central hole on the concave surface. The centroid–centroid separations of opposing benzene rings are 8.80 and 4.55 Å. A pharmacological study showed that the skeletal muscle relaxation activity is about 3.5 times less potent than that of *d*-tubocurarine. A comparison of the X-ray structure of marchantin A trimethyl ether and that of *O,O',N*-trimethyltubocurarine reported by Sobell *et al.* revealed that the molecules share almost the same macrocyclic bis(bibenzyl)ether skeleton structure, portions of which may therefore be crucial for the skeletal muscle relaxation activity.

Keywords marchantin A trimethyl ether; crystal structure; skeletal muscle relaxation activity; *d*-tubocurarine; *O,O',N*-trimethyltubocurarine

Marchantin A (MA)[1-6] (Fig. 1a), a novel macrocyclic bis(bibenzyl)ether, has been isolated from the liverwort *Marchantia* species, as a major component. Asakawa *et al.*[1] have reported that MA possesses cytotoxic, 5-lipoxygenase-inhibitory and calmodulin-inhibitory activities. Figure 1b shows the chemical structure of *d*-tubocurarine (*d*-TC), one of the curare alkaloids, which also contains a bis(bibenzyl)ether moiety as a part of bis(benzyltetrahydroisoquinoline) ether.[7] *d*-TC is a potent skeletal muscle relaxation agent,[8,9] being in clinical use. The actions of *d*-TC have been well defined: *d*-TC combines with the nicotinic cholinergic receptor at the postjunctional membrane in the motor end-plate and thereby inhibits competitively the transmitter action of acetylcholine. Two positive cationic nitrogen atoms separated by a distance of 13—15 Å are considered to be necessary to cause neuromuscular blockade.[8] Many competitive muscle relaxants carrying two cationic nitrogen atoms such as gallamine and pancuronium have been synthesized and employed clinically. During further studies of neuromuscular blockade, the non-competitive antagonistic action[10] of *d*-TC at higher concentrations and another mode of neuromuscular blockade involving compounds with no cationic nitrogen atom, such as lophotoxins, were found. The antagonistic actions of lophotoxins are competitive, but their actions are quite different from that of *d*-TC, since the relaxation is a result of irreversible covalent bonding to the receptor.[11] Attempts to analyze the structure–activity relationships have been made, but the role of the skeletal moiety of *d*-TC remains uncertain (it is noteworthy that *d*-TC is more potent than *l*-TC[9]). We felt that MA may possess skeletal muscle relaxation activity like that of *d*-TC, if the skeletal structure of *d*-TC is crucial for the activity, because of the structural similarity between MA and *d*-TC, *i.e.* (1) the ether linkages of rings A and C occur at the *ortho* and *meta* positions of the benzyl groups, respectively, (2) rings A and C are substituted by an OH or OCH_3 group at the *ortho* position to the ether linkages, (3) the linkages at rings B and D occur at the *meta* and *para* positions, though their actual positions are opposite, *i.e.*, the *meta* and *para* positions for *d*-TC, and the *para* and *meta* positions for MA, respectively.

In order to test this hypothesis, we performed an X-ray analysis of marchantin A trimethyl ether (MATE) and then studied its pharmacology, because MA itself was not available as crystals suitable for X-ray crystallography. The structure of *d*-TC has already been reported by Codding and James[12] and Reynolds and Palmer,[13] and the structure of its derivative, *O,O',N*-trimethyltubocurarine (TMTC), has been determined by Sobell *et al.*[14] We report here the molecular structure and pharmacological activities of MATE.

Experimental

Materials MATE was synthesized by methylation of MA.[5] *d*-TC and other compounds were purchased from Wako Co., Ltd. (Japan).

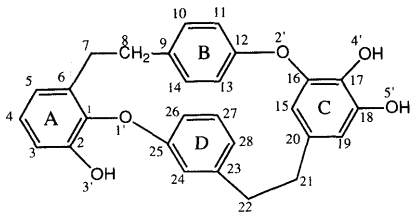

(a) marchantin A

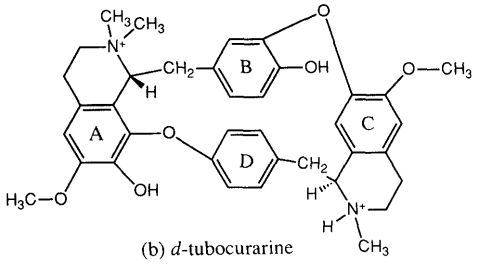

(b) *d*-tubocurarine

Fig. 1. The Chemical Structures of Marchantin A (a) and *d*-Tubocurarine (b), with the Atomic Numbering Scheme of Marchantin A

X-Ray Structure Determination Crystals of MATE were obtained by evaporation of an ethanol solution at room temperature. A single crystal with dimensions of $0.2 \times 0.15 \times 0.2\,mm^3$ was mounted on an automated Rigaku AFC-5B diffractometer using graphite-monochromated MoK_α radiation ($\lambda = 0.71069$ Å). Unit cell dimensions were determined by a least-squares fit of 2θ angles for 25 reflections ranging from $30° < 2\theta < 50°$.

TABLE I. Crystal Data and Experimental Details

Formula	$C_{31}H_{30}O_5$
Formula weight	482.575
Crystal system	Monoclinic
Space group	$P2_1/n$
a, Å	11.197 (4)
b, Å	18.600 (6)
c, Å	12.378 (4)
β, °	100.04 (3)
V, Å^3	2540.3 (15)
Z	4
D_x, g·cm^{-3}	1.262
μ(MoK_α), cm^{-1}	0.915
F(000)	1024
Data range measured	$0 \le h \le 13$, $0 \le k \le 20$, $-14 \le l \le 14$
No. of unique reflections	4916
No. of observed reflections (M)	2465 ($I > 3\sigma_I$)
No. of variables (N)	324
R	0.057
Rw	0.052
S	1.3340

TABLE II. Atomic Coordinates and Equivalent Thermal Parameters (B_{eq}/Å^2) of Non-hydrogen Atoms, with Estimated Standard Deviations in Parentheses for MATE

	x	y	z	B_{eq}
C(1)	0.1596 (4)	0.5366 (2)	0.8460 (3)	4.6
C(2)	0.2013 (5)	0.4751 (3)	0.9062 (3)	5.3
C(3)	0.1186 (6)	0.4237 (3)	0.9239 (4)	6.8
C(4)	−0.0019 (6)	0.4340 (3)	0.8851 (5)	7.4
C(5)	−0.0427 (5)	0.4967 (3)	0.8304 (4)	6.2
C(6)	0.0382 (4)	0.5495 (2)	0.8098 (3)	4.6
C(7)	−0.0072 (4)	0.6202 (3)	0.7622 (4)	5.7
C(8)	−0.0748 (4)	0.6199 (3)	0.6442 (4)	6.9
C(9)	0.0036 (4)	0.6310 (3)	0.5573 (4)	5.1
C(10)	0.0013 (5)	0.6970 (3)	0.5071 (4)	5.7
C(11)	0.0739 (4)	0.7114 (3)	0.4302 (4)	5.4
C(12)	0.1507 (4)	0.6582 (3)	0.4057 (3)	4.5
C(13)	0.1552 (4)	0.5928 (3)	0.4555 (4)	5.6
C(14)	0.0825 (5)	0.5793 (3)	0.5326 (4)	6.0
C(15)	0.3916 (4)	0.7005 (2)	0.4734 (3)	4.1
C(16)	0.3430 (4)	0.6860 (2)	0.3648 (3)	4.1
C(17)	0.4166 (4)	0.6860 (2)	0.2845 (3)	4.1
C(18)	0.5396 (4)	0.6985 (2)	0.3182 (3)	4.3
C(19)	0.5884 (4)	0.7125 (2)	0.4258 (3)	4.3
C(20)	0.5124 (4)	0.7133 (2)	0.5040 (3)	3.9
C(21)	0.5649 (4)	0.7266 (3)	0.6233 (4)	4.6
C(22)	0.6059 (4)	0.6573 (3)	0.6860 (4)	4.8
C(23)	0.5062 (4)	0.6042 (2)	0.6910 (3)	4.2
C(24)	0.4179 (4)	0.6181 (2)	0.7543 (3)	4.0
C(25)	0.3277 (4)	0.5683 (2)	0.7603 (3)	4.1
C(26)	0.3229 (4)	0.5042 (2)	0.7033 (3)	4.8
C(27)	0.4111 (5)	0.4905 (2)	0.6400 (4)	5.7
C(28)	0.5016 (5)	0.5395 (3)	0.6347 (4)	5.3
C(3′)	0.3711 (6)	0.4153 (4)	1.0118 (5)	10.0
C(4′)	0.3625 (5)	0.6053 (3)	0.1390 (4)	7.5
C(5′)	0.7310 (5)	0.7108 (3)	0.2619 (5)	7.6
O(1′)	0.2446 (3)	0.5875 (2)	0.8264 (2)	4.8
O(2′)	0.2224 (3)	0.6729 (2)	0.3260 (2)	5.6
O(3′)	0.3228 (4)	0.4725 (2)	0.9427 (3)	7.1
O(4′)	0.3666 (3)	0.6776 (2)	0.1761 (2)	5.5
O(5′)	0.6052 (3)	0.6967 (2)	0.2344 (2)	6.0

Intensity data were collected in the range of $2\theta < 50°$ with a $2\theta/\omega$ scanning mode. Three standard reflections were monitored for every 100-reflection interval and showed no significant time-dependence ($< \pm 2\%$). The background was counted for 5 s at both extremes of each peak. The observed intensities were corrected for Lorentz and polarization effects. No corrections for absorption and extinction effects were made. Experimental details of the X-ray study are given in Table I. The structure was solved by direct methods using the MULTAN program[15] and subsequently refined by a block-diagonal least-squares technique with the program REFINE/B in the program package X-STANP (written by one of us, Z.T.). The function minimized was $\Sigma w(|F_o| - |F_c|)^2$ with $w = 1.0$. All the hydrogen atoms were located on a difference map and were included in structure factor calculations with isotropic thermal parameters but not refined. In the final refinement, positional and anisotropic thermal parameters were varied for non-hydrogen atoms. The final agreement factors $R (= \Sigma(|F_o| - |F_c|)/\Sigma|F_o|)$ and $Rw (= [\Sigma w(|F_o| - |F_c|)^2/\Sigma w(|F_o|^2]^{1/2})$, and $S (= [\Sigma w(|F_o| - |F_c|)^2/(M-N)]^{1/2})$ are given in Table I. The residual electron density in the final difference Fourier

TABLE III. Bond Distances (Å) of MATE

C(1)–C(2)	1.400 (6)	C(16)–C(17)	1.398 (6)
C(1)–C(6)	1.376 (6)	C(16)–O(2′)	1.374 (5)
C(1)–O(1′)	1.393 (6)	C(17)–C(18)	1.387 (6)
C(2)–C(3)	1.375 (8)	C(17)–O(4′)	1.371 (4)
C(2)–O(3′)	1.358 (7)	C(18)–C(19)	1.374 (5)
C(3)–C(4)	1.365 (9)	C(18)–O(5′)	1.373 (5)
C(4)–C(5)	1.386 (8)	C(19)–C(20)	1.396 (6)
C(5)–C(6)	1.390 (7)	C(20)–C(21)	1.512 (6)
C(6)–C(7)	1.494 (6)	C(21)–C(22)	1.533 (7)
C(7)–C(8)	1.524 (6)	C(22)–C(23)	1.500 (7)
C(8)–C(9)	1.517 (7)	C(23)–C(24)	1.389 (6)
C(9)–C(10)	1.374 (8)	C(23)–C(28)	1.387 (7)
C(9)–C(14)	1.376 (8)	C(24)–C(25)	1.382 (6)
C(10)–C(11)	1.382 (8)	C(25)–C(26)	1.382 (5)
C(11)–C(12)	1.379 (7)	C(25)–O(1′)	1.389 (6)
C(12)–C(13)	1.361 (8)	C(26)–C(27)	1.387 (7)
C(12)–O(2′)	1.404 (5)	C(27)–C(28)	1.373 (8)
C(13)–C(14)	1.382 (8)	O(3′)–C(3′)	1.413 (8)
C(15)–C(16)	1.387 (5)	O(4′)–C(4′)	1.419 (7)
C(15)–C(20)	1.361 (6)	O(5′)–C(5′)	1.415 (6)

TABLE IV. Bond Angles (°) of MATE

C(2)–C(1)–C(6)	122.3 (4)	C(16)–C(17)–C(18)	117.6 (3)
C(2)–C(1)–O(1′)	118.2 (4)	C(16)–C(17)–O(4′)	120.4 (4)
C(6)–C(1)–O(1′)	119.4 (3)	C(18)–C(17)–O(4′)	121.9 (4)
C(1)–C(2)–C(3)	118.8 (5)	C(17)–C(18)–C(19)	122.0 (4)
C(1)–C(2)–O(3′)	115.4 (5)	C(17)–C(18)–O(5′)	113.7 (3)
C(3)–C(2)–O(3′)	125.9 (5)	C(19)–C(18)–O(5′)	124.3 (4)
C(2)–C(3)–C(4)	119.9 (5)	C(18)–C(19)–C(20)	119.2 (4)
C(3)–C(4)–C(5)	120.8 (6)	C(15)–C(20)–C(19)	120.1 (3)
C(4)–C(5)–C(6)	121.0 (5)	C(15)–C(20)–C(21)	119.9 (4)
C(5)–C(6)–C(1)	117.1 (4)	C(19)–C(20)–C(21)	120.0 (4)
C(5)–C(6)–C(7)	122.1 (4)	C(20)–C(21)–C(22)	112.9 (4)
C(1)–C(6)–C(7)	120.5 (4)	C(21)–C(22)–C(23)	114.5 (4)
C(6)–C(7)–C(8)	117.0 (4)	C(22)–C(23)–C(24)	120.6 (4)
C(7)–C(8)–C(9)	115.3 (4)	C(22)–C(23)–C(28)	120.9 (4)
C(8)–C(9)–C(10)	118.4 (5)	C(24)–C(23)–C(28)	118.5 (4)
C(8)–C(9)–C(14)	122.4 (5)	C(23)–C(24)–C(25)	120.3 (4)
C(10)–C(9)–C(14)	119.1 (5)	C(24)–C(25)–C(26)	121.0 (4)
C(9)–C(10)–C(11)	121.2 (5)	C(24)–C(25)–O(1′)	115.5 (3)
C(10)–C(11)–C(12)	118.5 (5)	C(26)–C(25)–O(1′)	123.5 (4)
C(11)–C(12)–C(13)	121.1 (4)	C(25)–C(26)–C(27)	118.6 (4)
C(11)–C(12)–O(2′)	118.0 (5)	C(26)–C(27)–C(28)	120.6 (4)
C(13)–C(12)–O(2′)	120.8 (5)	C(27)–C(28)–C(23)	121.0 (5)
C(12)–C(13)–C(14)	119.7 (5)	C(1)–O(1′)–C(25)	118.4 (3)
C(13)–C(14)–C(9)	120.3 (5)	C(12)–O(2′)–C(16)	115.9 (3)
C(20)–C(15)–C(16)	120.5 (4)	C(2)–O(3′)–C(3′)	119.0 (5)
C(15)–C(16)–C(17)	120.7 (4)	C(17)–O(4′)–C(4′)	114.2 (3)
C(15)–C(16)–O(2′)	124.7 (4)	C(18)–O(5′)–C(5′)	117.1 (3)
C(17)–C(16)–O(2′)	114.6 (3)		

map ranged from -0.32 to $0.41e \cdot Å^{-3}$. The calculations were performed by applications of the program packages RASA (Rigaku Co.), MULTAN and X-STANP on a mini-computer Micro VAX II. The atomic scattering factors used were taken from International Tables for X-Ray Crystallography.[16]

Pharmacological Activity of MATE The rectus abdominis muscle of a leopard frog (*Rana nigromaculata* HALLOWELL) (Japan SLC, Inc., Japan) was isolated, and the preparation was then immersed in a muscle bath filled with Ringer's solution. The composition of the Ringer's solution was: 0.6% NaCl, 0.0075% KCl, 0.01% $CaCl_2$, and 0.1% $NaHCO_3$. The pH of the solution was 7.7. The muscle bath was aerated from the bottom with air. The fluid in which the muscle was bathed was replaced by a solution containing acetylcholine bromide dissolved in the Ringer's solution. Cumulative dose–response curves were determined by means of a standard method.[17]

Results and Discussion

Molecular Structure of MATE The final atomic coordinates and equivalent thermal parameters for non-hydrogen atoms are listed in Table II. Bond distances and angles are given in Tables III and IV, respectively. The values are not significantly different from standard ones. A stereoscopic view of the molecule is shown in Fig. 2. It shows that MATE possesses convex and concave surfaces surrounded by four benzene rings, in which the plane of each benzene ring is roughly at right angles with those of the adjacent benzene rings. The ring centroid–centroid distances of MATE are 8.80 Å for A–C and 4.55 Å for B–D, and the distances between the neighboring rings are 5.60 Å for A–B, 4.79 Å for A–D, 4.76 Å for B–C and 4.74 Å and C–D.

To ascertain the similarity between the three-dimensional structures of MATE and *d*-TC, we compared the *d*-TC moieties in crystals of the dichloride, dibromide and TMTC diiodide salts with the structure of MATE. Reynolds and Palmer[13] have found that the conformations of the *d*-TC moieties in crystals of the dibromide and TMTC diiodide salts are similar, but that of *d*-TC dichloride is quite different, *i.e.*, the *d*-TC molecule in the dibromide salt takes a more open structure so that

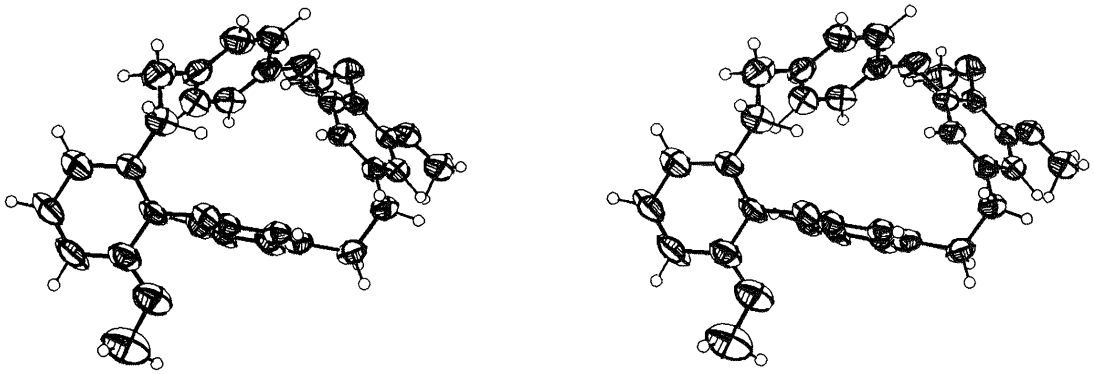

Fig. 2. Stereoscopic View of the Molecule of MATE, Showing Thermal Ellipsoids with 50% Probability

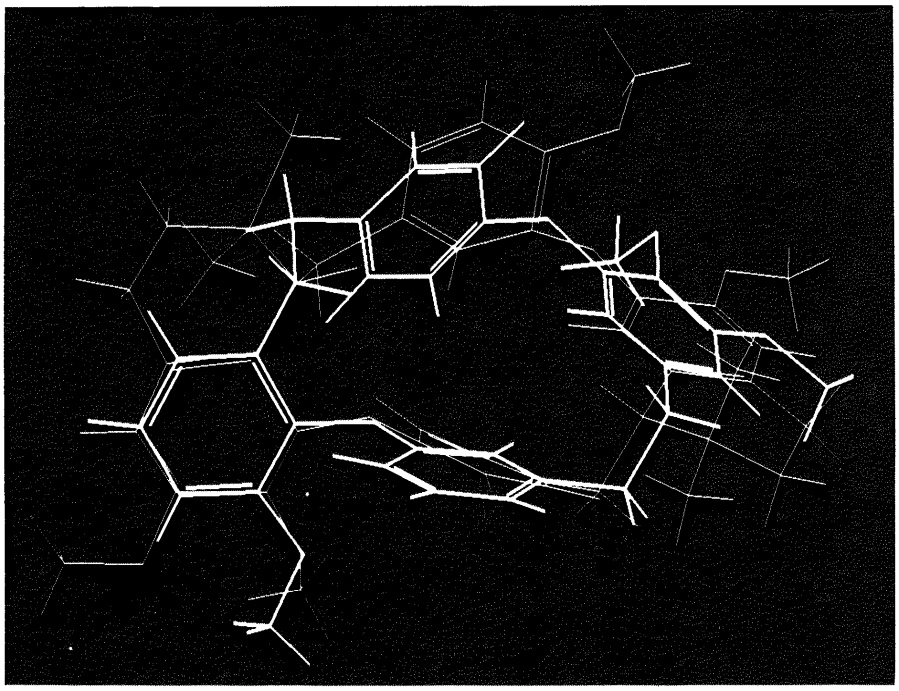

Fig. 3. Comparison of the X-Ray Structures of MATE and TMTC

The structure of TMTC (thin solid line) was superimposed on that of MATE (thick solid lines), then ring A was subjected to a least-squares fit. The structure of TMTC was reproduced from Sobell *et al.*, 1978.

the ring C rotates away from the center of the molecule relative to its position in the dichloride. Figure 3 shows that the conformation of MATE is similar to that of TMTC as a whole, in that the four benzene rings of MATE correspond to those of TMTC. The hole on the concave surface of MATE, was quite similar to that of TMTC, and the centroid–centroid separations between the four benzene rings of TMTC are 9.04 Å for A–C, 4.92 Å for B–D, 6.34 Å for A–B, 4.99 Å for A–D, 4.96 Å for B–C and 4.89 Å for C–D. As shown in Table V and Fig. 4, respectively, some of the dihedral angles between the four benzene rings and the torsion angles of the macrocyclic rings corresponded closely. The relative configuration around the carbon atom C(21) seemed to be different from that of the asymmetric carbon atom attached to ring C, and the dihedral and torsion angles around the atom were quite different. Nevertheless, the two molecules might be capable of binding to a common receptors in a common conformation, because the macrocycles are highly flexible, as demonstrated by NMR measurements of MATE[6] and TMTC.[18,19] Furthermore, as shown in Fig. 5, we found that the two surfaces of both molecules are very similar: a largely hydrophilic convex surface involving all the O atoms and an almost entirely hydrophobic concave

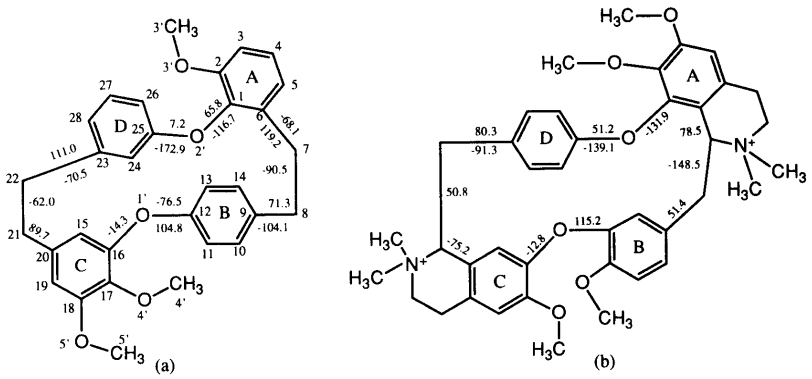

Fig. 4. Selected Torsion Angles (°) for MATE (a) and for TMTC (b)

TABLE V. Dihedral Angles (°) between the Benzene Rings A, B, C and D

Rings	MATE			TMTC		
	A	B	C	A	B	C
B	50.64			49.52		
C	70.45	82.43		47.13	93.58	
D	67.61	46.18	127.25	81.85	126.02	34.73

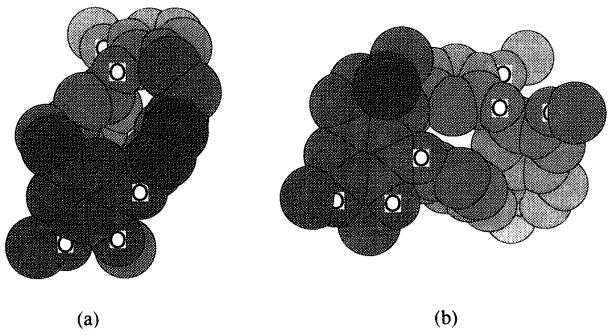

Fig. 5. The Hydrophilic Convex Surface with All O Atoms of MATE (a) and TMTC (b), Viewed Perpendicularly to Ring C of MATE and to Ring A of TMTC

For the sake of clarity, hydrogen atoms are omitted. The structure of TMTC was reproduced from Sobell *et al.*, 1978.

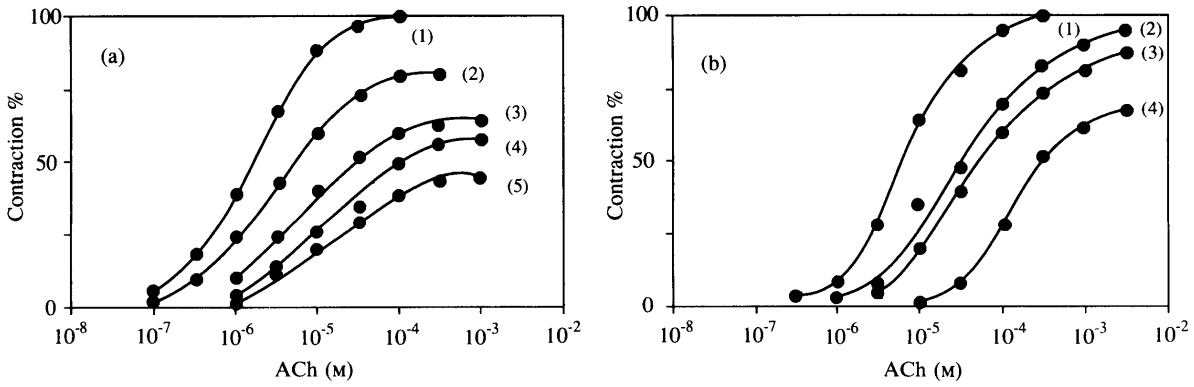

Fig. 6. Effects of MATE (a) and *d*-TC (b) on the Contractile Dose–Response Curves for Acetylcholine in the Rectus Abdominis of Frogs

Each point is the mean value for four experiments. Concentrations of MATE: (1) control, (2) 2×10^{-7}, (3) 2×10^{-6}, (4) 6×10^{-6} and (5) 2×10^{-5} M; concentrations of *d*-TC: (1) control, (2) 1×10^{-7}, (3) 1×10^{-6} and (4) 1×10^{-5} M.

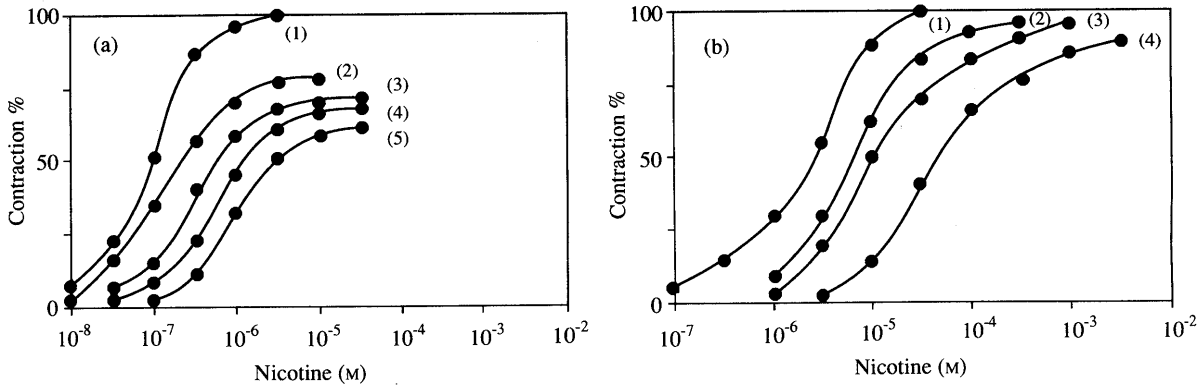

Fig. 7. Effects of MATE (a) and *d*-TC (b) on the Contractile Dose–Response Curves for Nicotine in the Rectus Abdominis of Frogs

Each point is the mean value for the four experiments. Concentrations of MATE: (1) control, (2) 2×10^{-7}, (3) 2×10^{-6}, (4) 2×10^{-5} and (5) 2×10^{-4} M; concentrations of *d*-TC: (1) control, (2) 1×10^{-7}, (3) 1×10^{-6} and (4) 1×10^{-5} M.

surface. Sobell *et al.*[14] have suggested that such a division of the molecule into hydrophilic and hydrophobic sides may be involved in the pharmacological activity of TMTC.

Pharmacological Activities of MATE and *d*-TC Figures 6 and 7 show the cumulative dose–response curves for the contracture induced by an agonist (ACh or nicotine) in the absence (control) or presence of MATE and *d*-TC, using the isolated rectus abdominis muscle of frogs. Additions of MATE shifted the curves to higher concentrations with simultaneous depression of the maximum activity. This indicated that MATE possesses a muscle relaxation activity and that its effect is competitive, although the actions of both MATE and *d*-TC appeared to involve antagonistic dualism at higher concentrations, as mentioned before. We further demonstrated that the activity is reversible, because relaxation activity recovered after washing the muscle with Ringer's solution (data not shown). Thus, the inhibitory mode of MATE was similar to that of *d*-TC. In order to compare the relaxation potency of MATE with *d*-TC, the apparent pA_2 values from Figs. 6 and 7 were calculated by means of the method of van Rossum[20]; for the contractures with ACh, 7.1 for MATE, 7.6 for *d*-TC; for those with nicotine, 6.7 for MATE, 7.2 for *d*-TC. Therefore, it is noteworthy that MATE, carrying no cationic nitrogen atom, possesses about 3.5 times less relative potency than *d*-TC. The value of pA_2 for *d*-TC was somewhat greater than reported values.[21,22]

We have as yet no direct evidence that the receptor for MATE is common with that for *d*-TC, and a further study will be necessary to establish this point.

References

1) Y. Asakawa, R. Matsuda, M. Toyata, C. Suire, T. Takemoto, R. Inoue, S. Hattori, M. Mizutani, *J. Hattori Bot. Lab.*, **50**, 165 (1981).
2) Y. Asakawa, M. Toyota, Z. Taira, T. Takemoto, M. Kido, *J. Org. Chem.*, **48**, 2164 (1983).
3) Y. Asakawa, M. Toyota, R. Matsuda, K. Takikawa, T. Takemoto, *Phytochemistry*, **22**, 1413 (1983).
4) Y. Asakawa, *J. Hattori Bot. Lab.*, **56**, 215 (1984).
5) Y. Asakawa, M. Tori, K. Takikawa, H. G. Krishnamurty, S. K. Kar, *Phytochemistry*, **26**, 1811 (1987).
6) M. Toyota, Thesis, Tokushima Bunri University, Tokushima, Japan, 1987, p. 9.
7) A. J. Everett, L. A. Lowe, S. Wilkinson, *J. Chem. Soc., Chem. Commun.*, **1970**, 1020.
8) M. M. Smith, "Drug Design," Vol. II, ed. by A. Arien, Academic Press, New York and London, 1971, p. 503.
9) P. Taylor, "The Pharmacological Basis of Therapeutics," 7th ed., ed. by A. G. Gilman, L. S. Goodman, T. W. Rall, F. Murad, Macmillan Publishing Co., New York, 1985, Chap. 11, p. 222.
10) D. Colquhoun, F. Dreyer, R. F. Sheridan, *J. Physiol.*, **293**, 247 (1979).
11) P. Culver, M. Burch, C. Potenza, L. Wasserman, W. Fenical, P. Taylor, *Mol. Pharmacol.*, **28**, 436 (1985).
12) P. W. Codding, M. N. G. James, *J. Chem. Soc., Chem. Commun.*, **1972**, 1174.
13) C. D. Reynolds, R. A. Palmer, *Acta Cryst.*, **B32**, 1431 (1976).
14) H. M. Sobell, T. D. Sakore, S. S. Tavale, F. G. Canepa, P. Pauling, T. J. Petcher, *Proc. Natl. Acad. Sci. U.S.A.*, **69**, 2212 (1972).
15) P. Main, L. Lessinger, M. M. Woolfsom, G. Germain, J. P. Declercq, MULTAN 77, A Program for the Automatic Solution of Crystal Structure from X-Ray Diffraction Data, University of York, England, 1977.
16) D. T. Cromer, J. T. Waber, International Tables for X-Ray Crystallography, Vol. IV, ed. by J. A. Ibers, W. C. Hamilton, Kynoch Press, Birmingham, 1974, p. 71.
17) H. Moritoki, M. Takei, M. Kotani, Y. Kiso, Y. Ishida, K. Endo, *Eur. J. Pharmacol.*, **100**, 29 (1984).
18) R. S. Egan, R. S. Stanaszek, D. E. Williamson, *J. Chem. Soc., Perkin Trans. 2*, **1973**, 716.
19) L. Koike, A. J. Marsaioli, F. de A. M. Reis, *J. Org. Chem.*, **46**, 2385 (1981).
20) J. M. van Rossum, *Arch. Int. Pharmacodyn.*, **143**, 299 (1963).
21) J. M. Bowen, *J. Pharmacol. Exp. Ther.*, **183**, 333 (1972).
22) E. F. van Maanen, *J. Pharmacol. Exp. Ther.*, **99**, 255 (1950).